Short-range attraction, surface currents, and mound formation in metal (111) epitaxial growth

Jianguo Yu and Jacques G. Amar

Department of Physics & Astronomy, University of Toledo, Toledo, Ohio 43606, USA
(Received 26 June 2003; revised manuscript received 17 November 2003; published 30 January 2004)

We present the results of molecular dynamics simulations of deposition near steps on Cu(111) and Ag(111) carried out in order to study the effects of short-range attraction in metal (111) epitaxial growth. Our results indicate that while short-range attraction plays an important role in the deposition of atoms near steps on (111) surfaces, there is a significant asymmetry between the interaction at A and B steps. These differences are explained in terms of the underlying geometry as well as the corresponding activation barriers. In particular, we find that due to short-range attraction the overall uphill funneling probability P_{av}^A and selected mound slope m_0^A for A steps are significantly *larger* than predicted by downward funneling. In contrast, the overall uphill funneling probability P_{av}^B and selected mound slope m_0^B for B steps are significantly lower than for A steps and appear to be close to the downward funneling prediction. In particular, atoms deposited near but somewhat beyond B steps have a lower uphill funneling probability than for A steps. In addition, for atoms deposited above the "upper terrace" of B steps we find that a new process, corresponding to the "knockout" of step-edge atoms, takes place leading to a reduced overall surface current and enhancing the asymmetry between A and B steps. General expressions for the surface current and selected mound slope which are valid for arbitrary crystal geometry for the case of irreversible growth with a large Ehrlich-Schwoebel barrier are also presented. These expressions are then used to analyze the implications of our results for unstable growth on (111) surfaces.

I. INTRODUCTION

One particularly important process controlling the evolution of the surface morphology is the accommodation of incoming atoms deposited near steps. For example, in metal epitaxial growth, the energy of condensation is believed to lead to "downward funneling" (DF),[1] i.e., atoms deposited beyond the edge of a step "funnel" to the bottom terrace, while atoms deposited on the "uphill" side go to the upper terrace. In the case of unstable growth, due either to an Ehrlich-Schwoebel (ES) barrier[2] to the descent of diffusing atoms at steps, or to step-adatom attraction,[3,4] or to step-edge diffusion,[5] the resulting balance between uphill and downhill currents leads to slope selection.[6] Analytical calculations[4] indicate that the surface current and selected mound slope depend strongly on the "bias" for atoms landing near a step.

Recently, we have shown[7] that for the case of metal (100) growth, the short-range attraction of depositing atoms to step edges can lead to significant deviations from the standard downward funneling picture for typical incident kinetic energies in epitaxial growth. In particular, we found that for Cu/Cu(100) and Ag/Ag(100), atoms deposited near close-packed step edges are significantly more likely to land on the upper terrace than predicted by downward funneling. As a result, in the case of unstable growth due to an ES barrier, the resultant uphill current can significantly enhance the selected mound angle and surface roughness.[7] In particular, by comparing kinetic Monte Carlo simulations of Cu/Cu(100) growth at $T = 160$ K with experiments,[8] we were able to show that uphill funneling due to short-range attraction can quantitatively explain both the experimentally observed mound slope [(113) facets] as well as the enhanced surface roughness at this temperature. We note that recent simulations of Ag/Ag(100) growth at low temperature[9] also demonstrate that short-range attraction can strongly enhance the

surface roughness, particularly at low incident kinetic energy. A comparison of our molecular dynamics results for deposition at Cu[110] steps obtained using an embedded-atom (EAM) potential[10] with the corresponding results obtained using a Lennard-Jones Cu potential[11] indicated that in this case the amount of uphill funneling depends relatively weakly on the details of the potential.

Here we investigate whether or not such effects also occur in metal fcc (111) epitaxial growth. In particular, we present the results of molecular dynamics simulations of deposition at A and B steps on Cu(111) and Ag(111), which were carried out in order to determine the effects of short-range attraction on uphill funneling and on the surface current. We note that mound formation has been observed in a variety of experiments on Cu/Cu(111) and Ag/Ag(111) growth.[12–16] In addition, a variety of theoretical and experimental studies[17–23] indicate that for metal (111) surfaces, the ES barrier for diffusion over descending step edges is relatively high compared to the barrier for diffusion on a flat terrace. Therefore, we expect that if short-range attraction leads to significant uphill funneling then this will have a significant effect on the surface morphology.

We note that there are two types of close-packed step edges on an fcc(111) surface: A steps corresponding to (100) microfacets and B steps corresponding to (111) microfacets (see Fig. 1). Therefore, in order to study the effects of short-range attraction we have carried out molecular dynamics simulations of deposition at both A and B step edges. For A steps, we find, as for the case of metal (100) growth,[7] that due to short-range attraction the "uphill funneling" probability P_{up}^A and surface current are significantly larger than predicted by the usual downward funneling picture. Similar results are obtained for the uphill funneling probability P_{up}^B for atoms deposited near but somewhat beyond a B step. However, due to the asymmetry between A and B steps, we find
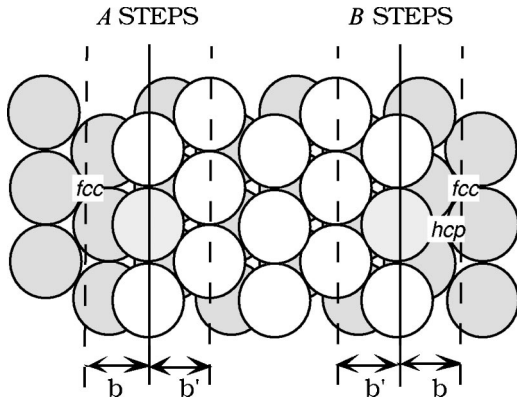
FIG. 1. Schematic diagram (top view) of A and B steps on a (111) surface.

that in general $P_{up}^A > P_{up}^B$. In addition, for atoms deposited above the "upper terrace" of B steps we find that a new process, corresponding to the "knockout" of step-edge atoms, takes place leading to a reduced overall surface current and a strong asymmetry between A and B steps. These differences between A and B steps are explained in terms of their geometry as well as the corresponding activation barriers. The implications of these results on the selected mound slopes and mound morphology are also discussed.

This paper is organized as follows. In Sec. II, we describe our molecular dynamics simulations in more detail. In Sec. III, we present our results and discuss the implications for the selected mound slopes and mound asymmetry in Cu/Cu(111) and Ag/Ag(111) growth. General expressions for the surface current and selected mound slope which are valid for *arbitrary crystal geometry* for the case of irreversible growth with a large Ehrlich-Schwoebel barrier are also presented. These expressions are then used to analyze the implications of our results on unstable growth on (111) surfaces. Finally, in Sec. VI we summarize our results. Detailed derivations of our general expressions for the surface current and selected mound angle are presented in the Appendix, along with illustrations for (100) and (110) surfaces.

II. MOLECULAR DYNAMICS SIMULATIONS

In order to determine the effects of short-range interactions we have carried out molecular dynamics (MD) simulations of adatom deposition at both A and B steps on both the Cu(111) and Ag(111) surfaces. As in our previous Cu(100) simulations,[7] in order to determine the effects of short-range attraction on atoms deposited near a step edge, we have measured the probability P_{up} that an atom deposited within a window (of size $b = \sqrt{3}a_1/2$ where a_1 is the nearest-neighbor distance, see Fig. 1) on the "downhill" side of the step-edge lands on the upper terrace. In order to take into account the possible effects of knockout, we have also measured the probability P'_{up} that an atom deposited within a window of size $b' = b$ on the uphill side of the step edge *remains* on the upper terrace. We note that the widths of the deposition windows were based on preliminary results which indicated that if an atom is deposited at a distance larger than b from the
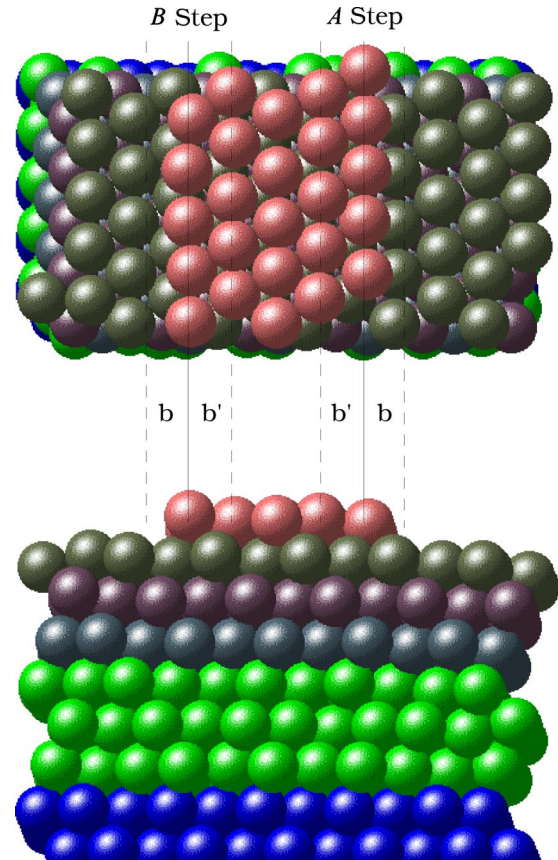

FIG. 2. Snapshots (side and top views) of the substrate configuration in MD simulations including both A and B steps.

step edge (see Fig. 1) then it always remains on the terrace on which it is deposited.

As in previous work[7] our simulations were carried out using EAM potentials for Cu and Ag (Ref. 10) since EAM potentials have been shown to be relatively accurate for metals. We note that we have recently found[24] that for deposition on Cu(100), the EAM potential-energy surface and steering forces are in relatively good agreement with static density-functional theory (DFT) calculations. Therefore, we expect that our EAM simulations will provide comparable accuracy in this case. In order to minimize finite-size effects, a system size of 10 1/2 layers was used, with each layer consisting of a terrace of 11 atoms by 5 atoms, while periodic boundary conditions were assumed along each terrace direction. As shown in Fig. 2, the top layer consists of an island of size 5 by 5 which has both an A step and a B step. As in our previous simulations of (100) deposition,[7] the top 3 1/2 layers underwent constant-energy molecular dynamics, while the bottom four layers were fixed. In order to equilibrate the substrate and absorb the energy of condensation of incoming atoms, the middle three layers of the system underwent constant temperature (Langevin) molecular dynamics.[25]

In our simulations, the system was first equilibrated at the desired temperature and the average position of the step edge was determined. Atoms were then deposited with the desired initial kinetic energy from an initial distance just above the potential cutoff and for each deposition the trajectory of the incoming atom was recorded. In order to study the depen-
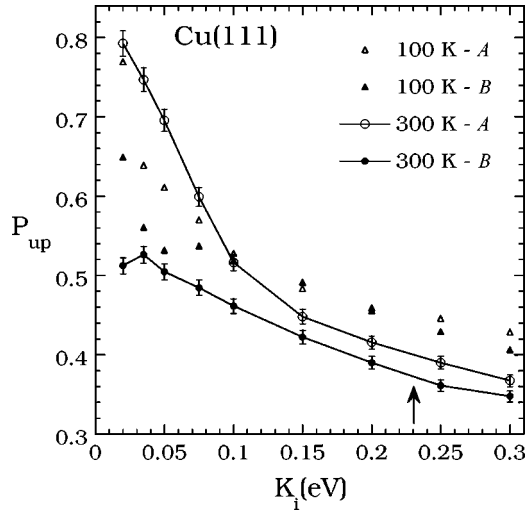
FIG. 3. Dependence of uphill funneling probability P_{up} on incident kinetic energy K_i for deposition at both A and B steps on Cu (111) surface (substrate temperature $T = 100$ K and 300 K). Arrow indicates average kinetic energy K_i of Cu atoms in epitaxial growth.

FIG. 4. Time evolution of trajectories and kinetic energies of deposited atom from the same position outside A (solid lines) and B (dashed lines) steps on Cu(111) surface with incident kinetic energy $K_i = 0.02$ eV and substrate temperature $T = 300$ K. Time interval for all trajectories is 2.4 ps.

dence on the incident energy K_i of the depositing atom, our simulations were carried out with K_i ranging from 0.02 eV to 0.3 eV. To obtain good statistics, 2500 depositions randomly distributed within each window were carried out for each value of the incident kinetic energy K_i. The time interval for each deposition was 2.4 ps for Cu(111) and 3.9 ps for Ag(111).

III. RESULTS

A. Uphill funneling probability P_{up} for atoms deposited above lower terrace

Figure 3 shows our results for the uphill funneling probability P_{up}^A for deposition beyond A steps and P_{up}^B for deposition beyond B steps on Cu(111) as a function of incident kinetic energy K_i for two different substrate temperatures ($T = 100$ K and 300 K). In the absence of short-range attraction the geometrical downward funneling picture holds and therefore one expects $P_{up} = 0$. However, as in the case of deposition on Cu(100), due to the short-range attraction there is significant uphill funneling (i.e., $P_{up} \neq 0$) for both A and B steps. In particular, for an incident kinetic energy corresponding to the average value expected in copper epitaxial growth ($\bar{K}_i = 2k_B T_m \simeq 0.23$ eV, where $T_m = 1356$ K is the melting temperature of copper) we find $P_{up}^A \simeq 0.45$ (0.40) and $P_{up}^B \simeq 0.44$ (0.38) for $T = 100$ (300) K. We note that in general $P_{up}^A > P_{up}^B$. In particular for small incident kinetic energy, P_{up}^A is significantly higher than P_{up}^B.

A priori, one might expect that the differences in the uphill funneling probabilities at A and B steps could be due to two different effects: (a) a difference in the strength of the steering effect at A and B steps and (b) differences in the interaction with the step after collision due to differences in the structure of A and B steps. In order to determine which is the dominant effect, we have compared the trajectories and kinetic energies for an atom deposited with very low incident
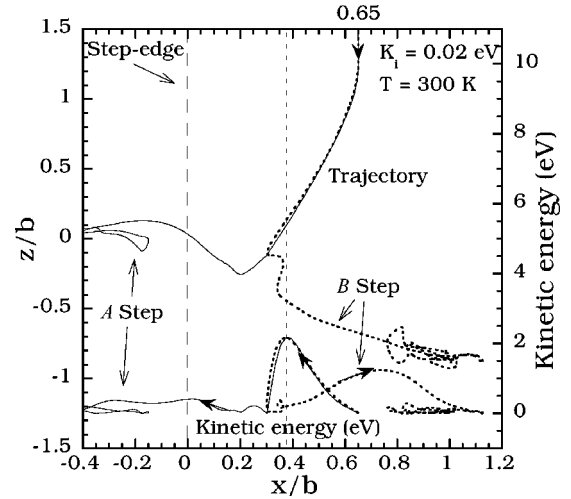
kinetic energy ($K_i = 0.02$ eV) at the same initial distance ($x_i/b = 0.65$) from the step edge, deposited at either an A step or a B step. As can be seen in Fig. 4, the steering effect is exactly the same for both A and B steps. However in the case of the B step, the depositing atom lands on the lower terrace, while in the the case of the A step the depositing atom lands on the upper terrace. This indicates that the difference in the uphill funneling probability is primarily due to differences in the step-adatom interaction after collision, which are due to a difference in the structure of A and B steps.

We note that these results may be explained by geometrical arguments. As can be seen in Fig. 1, while there is no difference between the intralayer interactions for edge atoms on A steps and those at B steps, there is an asymmetry in their interaction with the layer below during a collision with a depositing atom. In particular, motion of an edge atom at an A step towards the "uphill side" of the step involves passing through a "mid" site in the layer below towards the nearest hcp site. In contrast, the corresponding motion of an edge atom at a B step towards the uphill side of the step involves passing over an "atop" site. Therefore, as can be seen in Fig. 4, it is easier for an edge atom at an A step to be pushed downward towards the uphill side of the step than for an edge atom at a B step. As a result, depositing atoms colliding with an A step are more likely to reach the upper terrace than those colliding with a B step.

As shown in Fig. 5, similar results are found for Ag(111). As for the case of Cu(111), there is significant uphill funneling, i.e., $P_{up}^A \simeq 0.45$ and $P_{up}^B \simeq 0.35$, for an incident kinetic energy corresponding to the average value ($\bar{K}_i = 2k_B T_m \simeq 0.21$ eV) in Ag(111) epitaxial growth, while we again find that P_{up}^A is significantly higher than P_{up}^B. These results confirm that for deposition on metal (111) surfaces the standard downward funneling picture must be significantly modified to take into account the effects of short-range attraction.
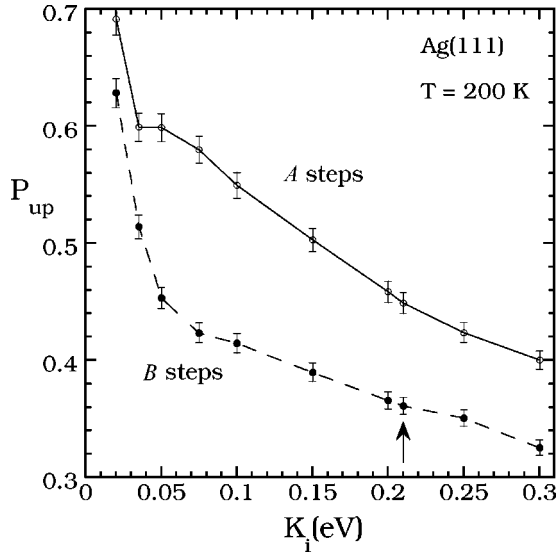
FIG. 5. Dependence of uphill funneling probability P_{up} on incident kinetic energy K_i for deposition at A and B steps on Ag (111) (substrate temperature $T = 200$ K). Arrow indicates average kinetic energy K_i of Ag atoms in epitaxial growth.

B. Uphill funneling probability P'_{up} for atoms deposited above upper terrace

We now consider the probability P'_{up} that an incident atom deposited on the *uphill* side of an A or B step *remains* on the upper terrace. According to the standard downward funneling picture, P'_{up} should always be equal to 1. As can be seen from Table I, for A steps this is indeed the case. However, for B steps we find $P'^B_{up} \simeq 1/2$, for Cu(111) and $P'^B_{up} \simeq 0.7$ for Ag(111), thus indicating that in both cases atoms deposited on the uphill side of a B step have a significant probability of arriving on the lower terrace.

In order to investigate this in more detail, we have measured the *local* uphill funneling probability $P(x) \, dx$ that an atom deposited at an initial distance x_i between x and $x + dx$ from a step edge lands on the upper terrace for a typical value of the incident kinetic energy $K_i \simeq 0.20$ eV in epitaxial Cu(111) growth. A positive value of x corresponds to deposition *beyond* the step edge, while a negative value corresponds to deposition on the uphill side. As can be seen in Fig. 6, for the case of A steps, atoms deposited on the uphill side almost always remain on the upper terrace, while for atoms deposited on the downhill side there is a critical distance ($\delta \simeq 0.35 \, b$) beyond which atoms almost always land

TABLE I. Dependence of uphill funneling probability P'_{up} on incident kinetic energy K_i for Cu(111) and Ag(111) A and B steps.

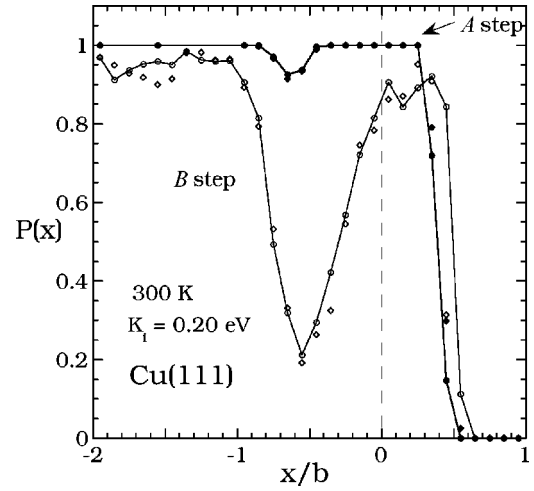| Metal	$K_i(eV)$	$P'_A(up)$	$P'_B(up)$
Cu(111)	0.15	0.98	0.51
300 K	0.20	0.98	0.54
	0.25	0.98	0.55
Ag(111)	0.20	0.97	0.71
200 K	0.25	0.96	0.68

FIG. 6. Local uphill funneling probability $P(x)$ for incoming atoms deposited at an initial distance x from a step edge ($T = 300$ K).

on the lower terrace. In contrast, for B steps there exists a relatively narrow range of negative values of x (corresponding to deposition on the upper terrace) at which the incident atom has a high probability of arriving on the lower terrace. As shown by the actual MD trajectories, this corresponds to an exchange process (knockout) in which the incident atom pushes out and replaces an atom on the step edge. In particular for $x \simeq -b/2$, which is halfway between the nearest hcp and fcc sites, the probability of remaining on the upper terrace is low. A summary of our results for the dependence of P'^B_{up} on the incident kinetic energy K_i for both Cu(111) and Ag(111) is shown in Fig. 7.

These differences in the behavior of A and B steps may be explained by the fact that, in qualitative agreement with recent DFT calculations for Cu(111),[26] for the EAM Ag(111) and Cu(111) potentials[10] used here, the barrier for exchange at B steps is significantly lower than at A steps.[27] The difference in the energy barriers for exchange at A and B steps may be explained by a simple geometric argument which applies when the barrier for terrace diffusion is sufficiently
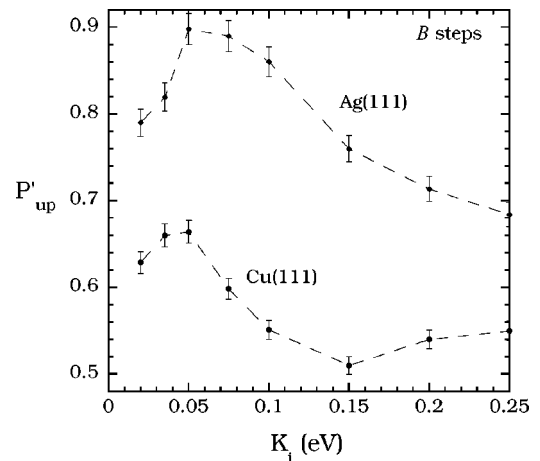

FIG. 7. Dependence of uphill funneling probability P'_{up} at B steps for Cu and Ag on incident kinetic energy K_i.
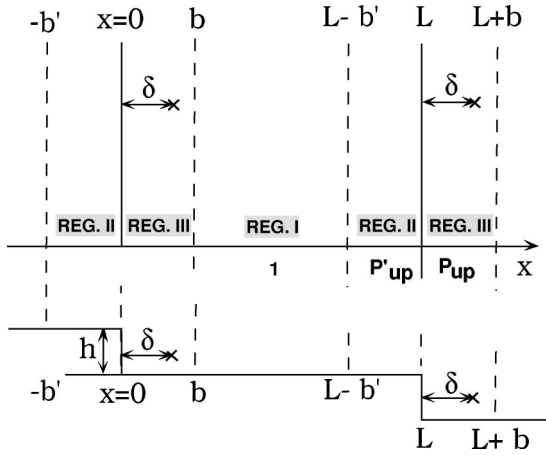
FIG. 8. Schematic showing steps (top and side view) on surface with terrace length L, step height h, attachment position δ, and window size b (b') on the lower (upper) terrace.

low. As can be seen in Fig. 1, for an A step-edge atom (shaded edge atom in Fig. 1) to arrive at the nearest fcc site, it must first travel over or near a relatively high-energy atop site, thus leading to a relatively high activation barrier for exchange. In contrast, a B step-edge atom (shaded edge atom in Fig. 1) may first move at relatively low-energy cost to the nearest hcp site, and then make a relatively low-energy barrier move to an fcc site. We note that in contrast, DFT calculations[28] indicate that for Pt(111) the barrier for exchange at B steps is *larger* than the barrier for exchange at A steps. This is due to the fact that for Pt(111) the barrier for hcp-fcc diffusion is quite high (0.35 eV).[28] Accordingly, the pathway for exchange diffusion at a step edge in Pt(111) is different from the one described here.

C. Implications for unstable growth

We now consider the consequences of our results on the selected mound slopes in unstable Ag (111) and Cu(111) epitaxial growth. As shown in the Appendix, for the case of irreversible growth (i.e., no detachment from steps) and a large ES barrier, one may use a continuum approach to obtain a general expression for the selected mound slope and surface current per particle J/F (where J is the surface current and F is the deposition flux) which is valid for arbitrary crystal geometry as a function of the step-height h, the terrace size L, the attachment position δ, the window sizes b and b', and the corresponding uphill funneling probabilities P_{up} and P'_{up} (see Fig. 8). In particular, we find

$$J/F = \frac{L^2 - 2L[\delta - bP_{up} + b'(1 - P'_{up})]}{2L}. \quad (1)$$

For the selected mound slope m_0, corresponding to the value of the terrace width L_0 for which the surface current is zero,[6] this implies the general result

$$m_0 = h/L_0 = \frac{h}{2[\delta - bP_{up} + b'(1 - P'_{up})]}. \quad (2)$$

For both A and B steps the step height is $h = a/\sqrt{3}$ (where a is the lattice constant), while the distance of the attachment site from the step edge is given by $\delta = \sqrt{6}\,a/4$. In our MD simulations we have used $b = b' = \delta$ and so from Eq. (2), we obtain

$$m_0^\alpha = \frac{\sqrt{2}}{6(1 - P_{av}^\alpha)}, \quad (3)$$

where $\alpha = A$ or B and $P_{av}^\alpha = (P_{up}^\alpha + P_{up}'^\alpha)/2$.

While the usual downward funneling assumption predicts $P_{av}^A = P_{av}^B = 1/2$ for A and B steps, our MD results for Cu(111) indicate $P_{av}^A \simeq 0.7$. Using Eq. (3) this implies a selected slope $m_0^A \simeq 0.8$ which is significantly higher than the DF prediction $m_0 \simeq 0.47$ and slightly higher than the slope of a (113) facet. In contrast, our results for Cu B steps ($P_{av}^B \simeq 0.45$) imply a maximum selected slope on B sides given by $m_0^B \simeq 0.43$, which is slightly lower than the DF prediction. Similarly for Ag(111), our MD results indicate $P_{av}^A \simeq 0.72$ which implies a selected slope $m_0^A \simeq 0.84$ which is again significantly higher than the DF prediction, while for B steps ($P_{av}^B \simeq 0.53$) we find $m_0^B \simeq 0.50$ which is again close to the DF prediction.

Thus, our results indicate that for irreversible Ag/Ag(111) and Cu/Cu(111) growth, the slopes on the A sides of mounds should be significantly larger than on the B sides. Accordingly, the resulting mounds should be strongly asymmetric. While we are not aware of an experiment in which the saturated mound slope(s) have been measured in Cu(111) unstable growth, scanning-tunneling microscopy pictures of the large-scale mounds formed during room-temperature growth of Ag/Ag(111) (Ref. 29) indicate the existence of significant anisotropy in agreement with our predictions. These results suggest that, while there are a number of other possible competing effects, the asymmetry in the interaction between depositing atoms and A and B step edges may play an important role in explaining the observed mound morphology.

IV. DISCUSSION

By carrying out molecular-dynamics simulations using EAM potentials, coupled with an analysis of the surface current, we have investigated the effects of short-range attraction on mound formation in metal (111) epitaxial growth. For both Ag(111) and Cu(111) our results indicate a significant asymmetry between the interaction of depositing atoms at A steps and B steps. In particular, we find that for A steps, due to the short-range attraction of depositing atoms to the step edge, the selected mound slope m_0^A and overall uphill funneling probability P_{av}^A are significantly *larger* than predicted by downward funneling. In contrast, due to the high probability of knockout or exchange at B steps, the overall uphill funneling probability P_{av}^B and selected mound slope m_0^B are significantly lower, and appear to be close to the downward funneling prediction. As already noted, these results imply a significant asymmetry in the mound shape for the case of unstable irreversible growth on metal (111) surfaces.

Using geometrical arguments, we have been able to ex-

plain these differences in the interaction of depositing atoms with A and B steps. In particular, geometrical differences appear to lead to two separate effects: (a) atoms depositing beyond a B-step edge are more likely to funnel to the lower terrace than those depositing beyond an A-step edge and (b) atoms depositing above the upper terrace of a B step are more likely to knock out a step-edge atom than those depositing above the upper terrace of an A step. In contrast to the usual exchange diffusion at a step edge, the energy required for the latter process is provided by the relatively high kinetic energy of condensation (approximately 2 eV) obtained by atoms depositing near a step edge.

As noted above, one particularly surprising result obtained in our simulations is the relatively high rate of knockout for atoms deposited near B steps. While our geometrical arguments indicate that the rate of knockout is significantly higher for B steps than for A steps, the exact rate for this process is likely to depend sensitively on the exchange barrier at B steps. In this connection, we note that Feibelman[26] has recently carried out density-functional-theory calculations of the exchange barriers for diffusion at Cu(111) A and B steps and obtained $E_{DFT}^A \simeq 0.34$ eV and $E_{DFT}^B \simeq 0.21$ eV with a barrier of 0.06 eV for hopping on a flat terrace. In contrast, the corresponding barriers obtained using the Cu(111) EAM potential used here are $E_{EAM}^A \simeq 0.32$ eV and $E_{EAM}^B \simeq 0.07$ eV with a barrier of 0.03 eV for hopping on a flat terrace.[27] Thus, while the qualitative behavior $E^B < E^A$ is the same for the EAM and DFT calculations, the DFT barrier for exchange at a B step is significantly larger than the corresponding EAM barrier.

These results suggest that the probability of knockout at a B step may actually be somewhat lower than indicated by our EAM simulations, and accordingly the correct uphill funneling probability $P_{up}^{\prime B}$ may be somewhat higher. However, we note that our EAM simulations for Ag(111), for which the EAM exchange barrier at a B step ($E_{EAM}^B \simeq 0.21$ eV) (Ref. 27) is essentially the same as the DFT Cu(111) prediction, still indicate a significant probability of knockout, i.e., $P_{up}^{\prime B} \simeq 0.7$. Thus, we expect that while knockout processes at B steps still play a significant role, the observed mound asymmetry for Cu(111) may be somewhat weaker than predicted by our EAM calculations.

In addition to our results for metal (111) epitaxial growth, we have also obtained general expressions for the surface current and selected mound slopes for the case of irreversible growth in the presence of a large ES barrier which take into account the short-range interaction of depositing atoms with steps. Using these results we have obtained explicit expressions for the surface current and selected mound angles for irreversible growth on the (100) and (110) surfaces of an fcc crystal as a function of the average uphill funneling probability. In the future, we expect that these results will be useful in further understanding the mound morphology and selected mound angles observed in metal epitaxial growth.

APPENDIX: CALCULATION OF SURFACE CURRENT

1. General calculation

In order to calculate the surface current as a function of slope for the case of a large ES barrier we use a quasi-one-dimensional approximation. In particular, we consider a regular periodic stepped surface with infinitely long straight monatomic height steps, terrace length L, step height h, and attachment position δ, where δ is the distance of an attachment site from the step edge. In order to take into account the interaction of depositing atoms with a step edge, we divide the terrace into three different regions as shown in Fig. 8. Particles deposited in region I ($b < x < L - b'$) are assumed to remain on the same terrace immediately following deposition. Particles deposited in region II ($L - b' < x < L$ or $-b' < x < 0$) are assumed to remain on the upper terrace with probability P_{up}'. Finally, particles deposited in region III ($0 < x < b$ or $L < x < L + b$) are assumed to have an overall probability P_{up} of arriving at the upper terrace.

The surface current per particle J/F (where J is the surface current and F is the deposition flux) may be calculated by integrating the distance particles must travel from their initial landing position to the attachment site at position δ multiplied by the probability of arriving at that site.[30] Accordingly, the total surface current per particle may be written as the sum of three terms J_1/F, J_2/F, and J_3/F, corresponding to each of the three regions. For a large step barrier, particles arriving in region I ($b < x < L - b'$) always attach to the upper step at position δ. Therefore, particles arriving at a distance x from the step-edge travel a distance $x - \delta$ and we may write

$$J_1/F = \frac{1}{L}\int_b^{L-b'} dx(x-\delta) = \frac{(L-b-b')(L+b-b'-2\delta)}{2L},$$
(A1)

where the factor $1/L$ arises from the fact that the probability that a particle lands in a particular interval dx is given by dx/L. Similarly, the second term may be written as

$$
\begin{aligned}
J_2/F &= \frac{1}{L}\int_{L-b'}^{L} dx(x-\delta)P'(x) \\
&\quad - \frac{1}{L}\int_{L-b'}^{L} dx(L-x+\delta)(1-P'(x)) \\
&= \frac{b'(LP_{up}'-\delta-b')}{L},
\end{aligned}
$$
(A2)

where $P'(x)dx$ represents the probability that a particle deposited in region II at a distance between x and $x + dx$ from the step edge will remain on the upper terrace (and thus travel a total distance $x - \delta$ to the upper attachment site),

while $(1-P'(x))dx$ is the probability that it will arrive on the lower terrace (and thus travel a total distance $L-x+\delta$ to the lower attachment site). The quantity $P'_{up} = (1/b')\int_{L-b'}^{L}P'(x)dx$ corresponds to the overall probability that an atom uniformly deposited in region II remains on the upper terrace immediately after deposition. We note that the usual assumption of downward funneling implies $P'_{up}=1$.

Finally, the third term may be written as

$$J_3/F = \frac{1}{L}\int_{L}^{L+b}dx(x-\delta)P(x)+(x-L-\delta)(1-P(x))$$

$$= \frac{b(2LP_{up}-2\delta+b)}{2L}, \qquad (A3)$$

where $P(x)dx$ represents the probability that a particle deposited at a distance between x and $x+dx$ from the step edge in region III will be attracted to the upper terrace due to short-range attraction (and thus travel a total distance $x-\delta$ to the upper attachment site), while $(1-P(x))\,dx$ is the probability that it will arrive on the lower terrace (and thus travel a total distance $x-L-\delta$ to the lower attachment site). The quantity $P_{up}=(1/b)\int_{L}^{L+b}P(x)dx$ corresponds to the overall probability that an atom uniformly deposited in the window $0<x<b$ lands on the upper terrace. We note that the usual assumption of downward funneling implies $P_{up}=0$.

Combining all three contributions, we obtain the following general expression for the surface current in the case of irreversible growth with a large step barrier as a function of terrace size L, attachment position δ, window sizes b and b', and the corresponding uphill funneling probabilities P_{up} and P'_{up}:

$$J/F = \frac{L^2-2L[\delta-bP_{up}+b'(1-P'_{up})]}{2L}. \qquad (A4)$$

The selected slope m_0 corresponds to the value of the terrace width L_0 for which the surface current is zero.[6] Accordingly one obtains

$$m_0 = h/L_0 = \frac{h}{2[\delta-bP_{up}+b'(1-P'_{up})]}. \qquad (A5)$$

We note that while Eq. (A5) applies strictly only to the case of a large Ehrlich-Schwoebel barrier E_{ES}, in previous work[4] we have calculated the selected slope as a function of E_{ES}/k_BT for the case of unstable growth on an fcc (100) surface. In this case, we found that the value of the selected mound slope was essentially independent of the barrier for $E_{ES}/k_BT>2$. Accordingly, we expect that Eq. (A5) should

provide an accurate estimate of the selected slope for the case of irreversible growth as long as $E_{ES}/k_BT>2$. For comparison with previous work, we now consider two specific cases in more detail.

2. fcc(100) surface

In this case the step height is given by $h=a/2$, where a is the lattice constant, while the attachment position is given by $\delta=a/\sqrt{2}$. Using these values along with window sizes $b=b'=\delta/2$ in Eq. (A5) we obtain the following general result:

$$m_0 = \frac{\sqrt{2}}{6-2(P_{up}+P'_{up})} = \frac{\sqrt{2}}{6-4P_{av}}, \qquad (A6)$$

where $P_{av}=(P_{up}+P'_{up})/2$. We note that in this case, calculations of the surface current have previously been carried out[4,7,31,32] using discrete sums over attachment sites along with the assumption that $P'_{up}=1$. In molecular dynamics simulations of deposition on Cu(100) and Ag(100), (Ref. 7) we also found $P'_{up}=1$. Substituting this value in Eq. (A5) we obtain

$$m_0 = \frac{\sqrt{2}}{4-2\,P_{up}} \qquad (A7)$$

in agreement with our previous work.[4,7]

3. fcc(110) surface

Due to anisotropy, for the case of growth on an fcc(110) surface, there are two types of step edges—one along the $[1\bar{1}0]$ direction and the other along the $[100]$ direction, while $h=\sqrt{2}a/4$ (where a is the lattice constant). For both cases, we assume $b=b'=\delta$, where δ is the distance of the attachment site from the step edge. We then obtain for the selected slope

$$m_0 = \frac{h/\delta}{4(1-P_{av})}, \qquad (A8)$$

where $P_{av}=(P_{up}+P'_{up})/2$.

For the $[1\bar{1}0]$ step, $\delta=a$, which implies

$$m_0^{[1\bar{1}0]} = \frac{\sqrt{2}}{16(1-P_{av})}. \qquad (A9)$$

Similarly for the $[100]$ step, $\delta=a/\sqrt{2}$ which implies

$$m_0^{[100]} = \frac{1}{8(1-P_{av})}. \qquad (A10)$$

[1] J.W. Evans, D.E. Sanders, P.A. Thiel, and A.E. DePristo, Phys. Rev. B **41**, 5410 (1990); H.C. Kang and J.W. Evans, Surf. Sci. **271**, 321 (1992).

[2] G. Ehrlich and F. Hudda, J. Chem. Phys. **44**, 1039 (1966); R.L. Schwoebel, J. Appl. Phys. **40**, 614 (1969).

[3] S.C. Wang and G. Ehrlich, Phys. Rev. Lett. **70**, 41 (1993).

[4] J.G. Amar and F. Family, Phys. Rev. B **54**, 14 071 (1996); Phys. Rev. Lett. **77**, 4584 (1996).

[5] M.V. Ramana Murty and B.H. Cooper, Phys. Rev. Lett. **83**, 352 (1999).

[6] M. Siegert and M. Plischke, Phys. Rev. Lett. **73**, 1517 (1994); Phys. Rev. E **53**, 307 (1996).

[7] Jianguo Yu and Jacques G. Amar, Phys. Rev. Lett. **89**, 286103 (2002).

[8] H.-J. Ernst, F. Fabre, R. Folkerts, and J. Lapujoulade, Phys. Rev. Lett. **72**, 112 (1994).

[9] F. Montalenti and A.F. Voter, Phys. Rev. B **64**, 081401(R) (2001); F. Montalenti, M.R. Sorensen, and A.F. Voter, Phys. Rev. Lett. **87**, 126101 (2001).

[10] A.F. Voter, Proc. SPIE **821**, 214 (1987); Report No. LA-UR 93-3901, 1993 (unpublished).

[11] D.E. Sanders and A.E. DePristo, Surf. Sci. **254**, 341 (1991).

[12] W.C. Elliott, P.F. Miceli, T. Tse, and P.W. Stephens, Phys. Rev. B **54**, 17 938 (1996); Physica B **221**, 65 (1996); in *Surface Diffusion: Atomistic and Collective Processes*, Vol. 360 of *NATO Advanced Studies Institute, Series B: Physics*, edited by M.C. Tringides (Plenum, New York, 1997), p. 209.

[13] J. Alvarez, E. Lundgren, X. Torrelles, and S. Ferrer, Phys. Rev. B **57**, 6325 (1998).

[14] C.E. Botez, P.F. Miceli, and P.W. Stephens, Phys. Rev. B **64**, 125427 (2001).

[15] C.E. Botez, W.C. Elliott, P.F. Miceli, and P.W. Stephens, in *Mechanisms of Surface and Microstructure Evolution in Deposited Films and Film Structures*, edited by J. Sanchez, Jr., J.G. Amar, R. Murty, and G. Gilmer, Mater. Res. Soc. Symp. Proc. No. 672 (Materials Research Society, Pittsburgh, 2001), p. O1.5.

[16] C.E. Botez, W.C. Eliott, P.F. Miceli, and P.W. Stephens, in *Mechanisms of Surface and Microstructure Evolution in Deposited Films and Film Structures*, edited by J. Sanchez, Jr., J.G. Amar, R. Murty, and G. Gilmer, Mater. Res. Soc. Symp. Proc. No. 672 (Materials Research Society, Pittsburgh, 2001), p. O2.7.

[17] K. Bromann, H. Brune, H. Roder, and K. Kern, Phys. Rev. Lett. **75**, 677 (1995).

[18] G. Schulze Icking-Konert, M. Giesen, and H. Ibach, Surf. Sci. **398**, 37 (1998).

[19] M. Giesen and H. Ibach, Surf. Sci. **431**, 109 (1999).

[20] O.S. Trushin, K. Kokko, P.T. Salo, W. Hergert, and M. Kotrla, Phys. Rev. B **56**, 12 135 (1997).

[21] Y. Li and A.E. DePristo, Surf. Sci. **319**, 141 (1994).

[22] K.R. Roos and M.C. Tringides, Phys. Rev. Lett. **85**, 1480 (2000).

[23] K. Morgenstern *et al.*, Phys. Rev. Lett. **80**, 556 (1998).

[24] J. Yu, J.G. Amar, and A. Bogicevic (unpublished).

[25] J. Jacobsen, B.H. Cooper, and J.P. Sethna, Phys. Rev. B **58**, 15 847 (1998).

[26] P.J. Feibelman, Phys. Rev. Lett. **85**, 606 (2000); Surf. Sci. **478**, L349 (2001).

[27] C. Ghosh, S. Durukanoglu, A. Kara, and T. S. Rahman (unpublished).

[28] P.J. Feibelman, Phys. Rev. Lett. **81**, 168 (1998).

[29] J. Vrijmoeth, H.A. van der Vegt, J.A. Meyer, E. Vlieg, and R.J. Behm, Phys. Rev. Lett. **72**, 3843 (1994).

[30] Here we assume that the diffusion length l_D is sufficiently large compared to the terrace width L, that all particles deposited on a terrace attach to the ascending step rather than nucleating or attaching to an island. For a large step barrier, and L close to the selected terrace width L_0, this is a reasonable assumption.

[31] J.G. Amar and F. Family, Phys. Rev. B **54**, 14 742 (1996).

[32] M.C. Bartelt and J.W. Evans, Surf. Sci. **423**, 189 (1999).